RSC Advances

PAPER

View Article Online
View Journal | View Issue

Cite this: *RSC Adv.*, 2017, **7**, 55215

Nanosilica-supported thiosemicarbazide–glutaraldehyde polymer for selective Au(III) removal from aqueous solution

Gengwei Zhang,[b] Yang Zhou,[a]* Zhao Ding,[c] Likang Fu[b] and Shixing Wang*[b]

Received 13th September 2017
Accepted 29th November 2017

DOI: 10.1039/c7ra10199f

rsc.li/rsc-advances

A new adsorbent thiosemicarbazide/nanosilica composite was synthesized *via* a facile two-step reaction, including the functionalization of silica nanoparticles *via* amino groups, and crosslinking the thiosemicarbazide with glutaraldehyde onto the amino functionalized silica nanoparticles. The adsorption capability of the adsorbent for Au(III) ions was investigated. Fourier transform infrared, X-ray photoelectron spectroscopy and thermogravimetric analysis were used to characterize the adsorbent. Experimental results indicated that nanocomposites exhibited highly selective and efficient adsorption for Au(III). The equilibrium data fitted well with the Langmuir isotherm and the obtained kinetic data obeyed the pseudo-second-order kinetics model. The maximum adsorption capacity was 4.3 mmol g^{-1} at pH 2. The adsorbent can still keep high adsorption capability after five recycling rounds. The adsorption mechanisms were proposed as the synergistic effect of ionic interaction and chelation.

1. Introduction

Gold is one of the precious metals that has been widely used in high-tech industries, catalysts in various chemical processes, electrical and electronic industries, agriculture and medicine.[1] The need for recycling or recovery of Au(III) economically has increased due to the increases in industrial demand and its value. The detection and recovery of Au(III), however, are not simple issues because of its low concentration in environmental, geological and metallurgical materials. So there is a strong economic motivation for the recovery of Au(III) from aqueous solution. Some methods such as solvent extraction,[2] adsorption,[3] precipitation[4] and membrane separation[5] have been reported for the recovery of gold from aqueous solutions. Among these methods, adsorption is regarded as an effective technology due to its low energy consumption, low cost, ease of operation and high efficiency.

A good adsorbent should consist of a stable matrix and suitable groups. Amino groups are usually utilized as efficient chelating groups for recovery of Au(III).[6–8] In recent years, chelating resins with various functional groups have been widely used for recovery of gold due to their high selectivity.[9] The resins containing groups with nitrogen or sulphur atom can selective chelating with precious metals according to Pearson's hard soft acid–base theory.[10] However, there are some disadvantages of resin matrix, such as swelling, sensitivity to chemical environment and low mechanical stability.[11] Inorganic supports, therefore, are suggested to take place of resin matrix due to advantages of no swelling and good mechanical stability. Furthermore, inorganic substrate can get unique opportunities by immobilizing of organic functional groups.[12] Among different inorganic supports, nanosilica is known to be one of the most ideal materials due to its advantages of reliable chemical, mechanical and thermal stability, economy, extremely large surface area, short diffusion distance and facile surface modification.[13,14]

In this study, thiosemicarbazide/nanosilica composite (TSC–SNC) was synthesized *via* crosslinking the thiosemicarbazide with glutaraldehyde onto the surface of the amino functionalized silica nanoparticles. We investigated systemically the adsorption properties such as selective capture in coexisting other metal ions solution, adsorption efficiency with different pH value and recycling times for Au(III). The adsorption mechanism, adsorption kinetics and isotherms were also discussed to support the proposal of synergistic effect of ionic interaction and chelation.

2. Experimental section

2.1. Chemicals

Silica nanoparticles (SNPs), 3-aminopropyltriethoxysilane (APTES) and thiosemicarbazide (TSC) were obtained from Aladdin-reagent Co., Ltd. Ethanol and glutaraldehyde (GTA) were obtained from Tianjin Chemical Regents, Inc. All reagents

[a]*School of Textile Science and Engineering, National Engineering Laboratory for Advanced Yarn and Clean Production, Wuhan Textile University, Wuhan 430200, China. E-mail: zhouyangnano@163.com*

[b]*Faculty of Metallurgical and Energy Engineering, Kunming University of Science and Technology, Kunming 650093, China. E-mail: wsxkm@sina.com*

[c]*Department of Mechanical, Materials and Aerospace Engineering, Illinois Institute of Technology, Chicago 60616, USA*

were analytical grade. Metal solutions were prepared by diluting standard solutions with distilled water. These stock solutions were adjusted to the desired pH values by adding HCl or NaOH solutions.

2.2. Preparation of TSC–SNC adsorbent

The preparation process of the adsorbent was presented in Scheme 1. SNPs (3.0 g), ethanol (50 mL) and APTES (6 mL) were added to a 250 mL three-necked flask. The suspension was stirred and refluxed for 18 h. Then the solid was separated by centrifugation, washed with ethanol and dried to give APTES–SNPs. In the next step, for preparation thiosemicarbazide/silica nanocomposite, 2.8 g of APTES–SNPs was dispersed in 50 mL distilled water in a 250 mL three-necked flask, followed by addition of TSC (6 g) and GTA (10 mL). The solution was adjusted to pH 8 using ammonia and stirred at 90 °C for 9 h. The resulting final product (TSC–SNC) was washed with deionized water and dried under vacuum.

2.3. Adsorption experiments

All gold adsorption experiments were performed in a thermostat steam bath vibrator at a shaking speed of 240 rpm at 25 °C. The adsorption amount (q, mmol g^{-1}) of metal ions on the adsorbent and adsorption percent (R, %) were measured by the formula:

$$q = V(C_0 - C_t)/m \quad (1)$$

$$R = (C_0 - C_t)/C_t \quad (2)$$

where V (L) is the volume of Au(III) solution and m (g) represents the mass of TSC–SNC. C_0 and C_t (mmol L^{-1}) are the initial and final concentration of Au(III) solution, respectively. All adsorption experiments were performed in three replicates.

To evaluate the effect of pH, 20 mg of TSC–SNC was added into a series of flasks containing 200 mL solutions at 100 mg L^{-1} Au(III) concentration, the initial pH was adjusted using NaOH and HCl solution to the designated values from 2 to 10. The experiments were performed for 5 h and then the concentration of Au(III) in the solutions was determined.

To evaluate the selectivity of TSC–SNC, 20 mg of TSC–SNC was added into 200 mL solutions containing a mixture of Au(III), Cu(II), Zn(II) and Pb(II) at pH 2. The initial concentration of the coexisting metal ion is 100 mg L^{-1}, respectively. The mixtures were shaken for 5 h, then the concentrations of the coexisting metal ion in the solutions were determined.

For adsorption isotherms, 20 mg of TSC–SNC was added into a series of flasks containing 200 mL solutions at pH 2, the initial Au(III) concentration varied in the range of 80 to 160 mg L^{-1}. The mixtures were shaken for 5 h, and the concentration of Au(III) in the solutions was determined.

Adsorption kinetics experiments were performed by adding 20 mg of TSC–SNC into a series of flasks containing 200 mL solutions at pH 2 and 100 mg L^{-1} Au(III) concentration. The concentration of Au(III) in solutions after different time intervals (2–120 min) was determined.

The recycling was tested by adding 20 mg of TSC–SNC to a flask containing 200 mL solutions at pH 2 and 100 mg L^{-1} Au(III) concentration. After 5 h shaking, the concentration of Au(III) in the solutions was determined. The Au loaded TSC–SNC was separated and then oscillated for 5 h with 0.1 M thiourea and 0.1 M HNO_3 solution. The adsorbent was then washed with distilled water, dried and reused in adsorption experiment. The whole process repeated 5 times by using the same adsorbent.

2.4. Characterization

FTIR was recorded on a FTIR spectrometer (Bruker, Equinox55, Germany). XPS analyses were performed with an electron spectrometer (VG Scientific, ESCALab220i-XL, UK). TGA measurements were conducted on PerkinElmer TGA-7 (USA) thermogravimetric analyzer at a heating rate of 10 °C min^{-1}. After adsorption, the supernatant was collected and analyzed by inductively coupled plasma atomic emission spectrometry (ICP-AES) (Leema, Prodigy 7, USA). The zeta potential of TSC–SNC in the aqueous solution was analyzed on a Zeta Plus potentiometer (Brookhaven, USA).

3. Results and discussion

3.1. Characterization of TSC–SNC

Fig. 1 shows the FTIR spectra of SNPs, APTES–SNPs and TSC–SNC. In the spectra of SNPs, The peak at 3430 cm^{-1} and 1633 cm^{-1} were due to the O–H stretching vibration and the O–H bending vibration of the adsorbed water and silanol groups. The adsorption peak at 1110 cm^{-1} was corresponded to the Si–O–Si asymmetric stretching vibrations, and the peaks at 800 and 474 cm^{-1} were attributed to the Si–O–Si symmetric stretching vibrations and bending vibrations, respectively. For APTES–SNPs, the C–H stretching vibration at 2924 cm^{-1} and

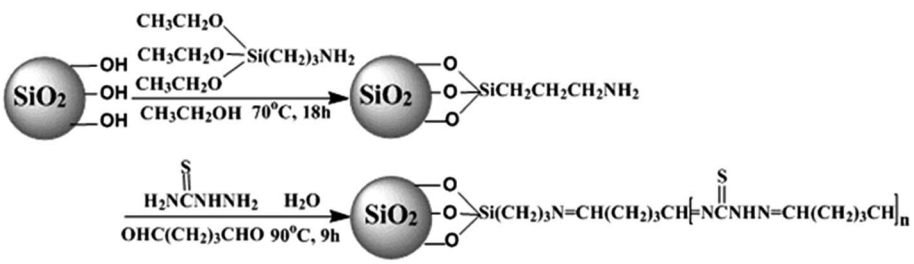

Scheme 1 Preparation process of TSC–SNC adsorbent.

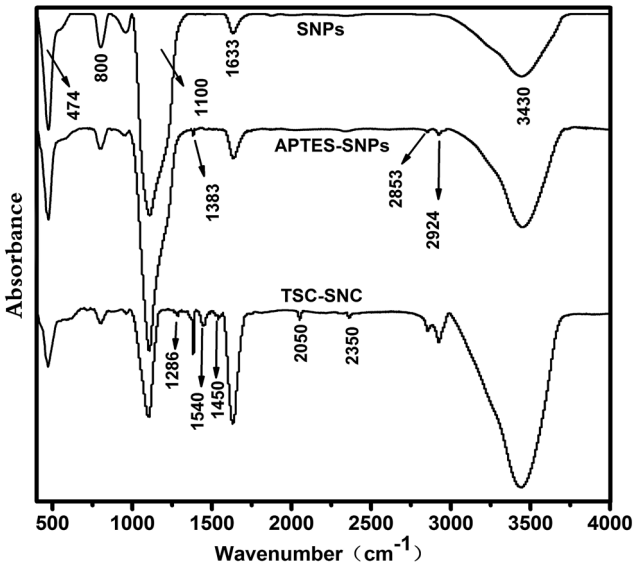

Fig. 1 FT-IR spectra of SNPs, APTES–SNPs and TSC–SNC.

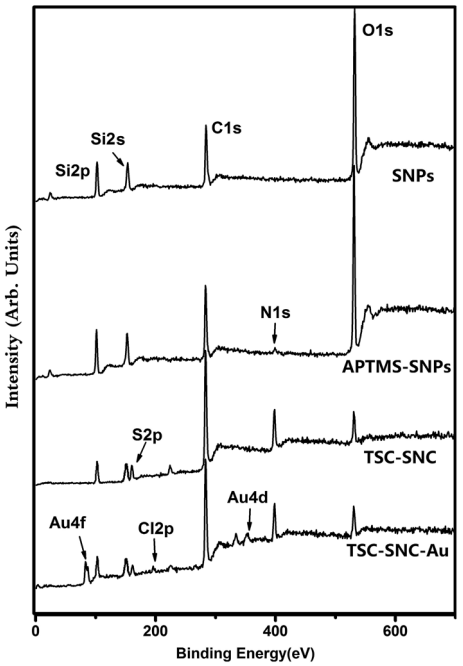

Fig. 2 XPS survey scan of SNPs, APTES–SNPs, TSC–SNC and TSC–SNC–Au.

2853 cm^{-1}, and the $-CH_3$ bending vibrations at 1383 cm^{-1} demonstrated the organic silane had been successfully grafted on the surface of silica nanoparticles.

In the spectra of TSC–SNC, the peaks at 1286, 1450 and 1540 cm^{-1} came from N–C=S, C–N and C=N bonds, respectively. The new peaks at 2050 and 2345 cm^{-1} were corresponded to $C{=}NH^+$ and S–H bonds respectively attributing to the thione–thiol tautomerism of thioamide groups.[15] In addition, the peaks at 1633 and 3430 cm^{-1} were broader owing to the overlap of the peaks of N–H stretching and bending vibration and the O–H stretching vibration.

X-ray photoelectron spectroscopy was used to clarify the chemical composition of the composites. Fig. 2 shows the wide-scan spectra for these samples. The characteristic peaks of O 1s, C 1s, Si 2p and Si 2s were observed in the spectra of SNPs. In comparison with SNPs, the nitrogen peak at 401.2 eV was observed in the spectrum of APTES–SNPs. The spectra of TSC–SNC presented S 2p signal at 168.2 eV, which arose from the thioamide group. In order to clarify the elemental composition, we measured the XPS spectra of C 1s (Fig. 3). The C 1s signal of APTES–SNPs presented two peaks at 284.6 and 286.2 eV, corresponded to C–C(H) and C–N species. The C 1s of TSC–SNC can be curve-fitted into five peak components. The new peaks at 285.9, 287.9 and 288.5 eV are corresponded to C–S, C=N and C=S species, respectively, which confirms that thiosemicarbazide–glutaraldehyde has been successfully grafted on the silica nanoparticles.

Fig. 4 shows the TGA analysis of the SNPs, APTES–SNPs and TSC–SNC. The mass loss of TSC–SNPs was 67.7%. While the unfunctionalized SNPs and APTMS–SNPs only show mass losses of 9.1% and 13.3%, respectively. The mass loss was due to the evaporation of water and decomposition of organic molecules. Based on the TGA curves in Fig. 4, the amount of the thiosemicarbazide–glutaraldehyde polymer in the composite was calculated to be 54.4 wt%.

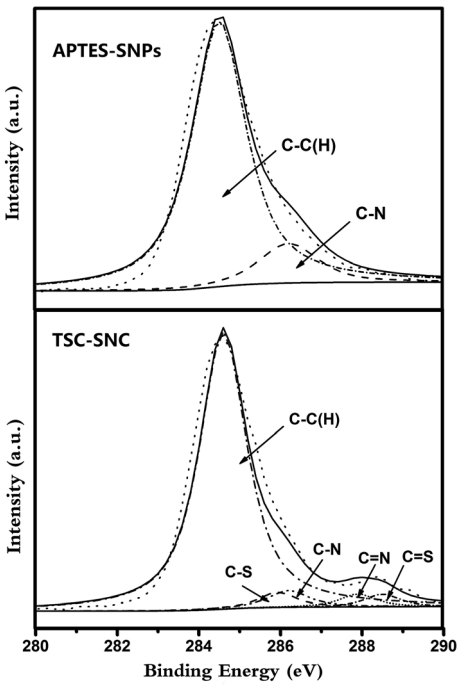

Fig. 3 The C 1s spectra of APTES–SNPs and TSC–SNC.

3.2. Adsorption behavior of TSC–SNC

3.2.1 The effect of pH on adsorption Au(III). The effect of different pH value from 2 to 10 on Au(III) adsorption was studied. At low pH, gold forms $AuCl_4^-$ complex ions in chloride solution, and chloride–hydroxide complexes of Au(III) begin to form when pH is above 4.[16] Fig. 5 shows that adsorption

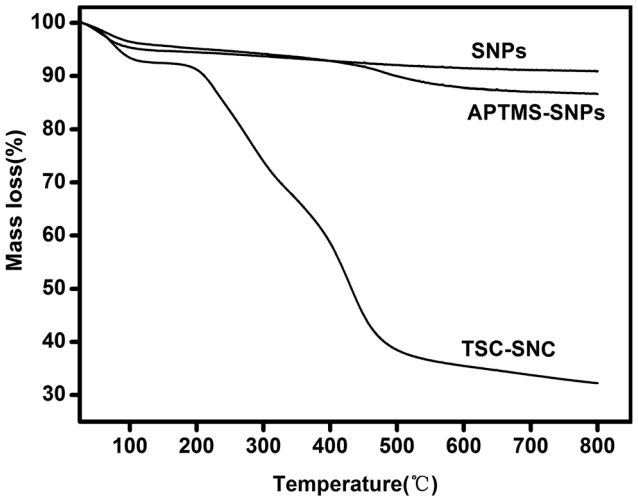

Fig. 4 TGA of SNPs, APTES–SNPs and TSC–SNC.

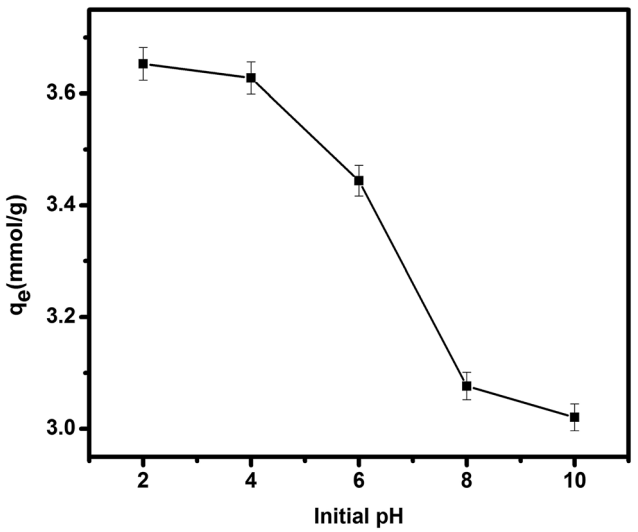

Fig. 5 The effect of pH on the adsorption of Au(III), TSC–SNC = 20 mg, $[Au^{3+}] = 100$ mg L^{-1}, adsorption time = 5 h.

capacity markedly decreased with an increase of pH value of the solution. The optimal pH for the recovery of Au(III) was around 2. Fig. 6 shows the effect of pH on zeta potential of TSC–SNC. The zeta potential of TSC–SNC decreased with the increasing of pH value. At pH = 2, TSC–SNC was positively charged. So most of the amine and thioamide groups on the adsorbent surface were protonated and the adsorbent acquired positively charged surface at low pH, which enhanced the electrostatic attraction between $AuCl_4^-$ and the adsorbent.

3.2.2 Adsorption selectivity. Au(III) often coexists with other metal ions in aqueous solutions. The investigation of selective adsorption of the TSC–SNC for Au(III) is therefore necessary. To test whether the specificity in the adsorption of Au(III) is compromised by complex mixtures of other cations, we used the interfere medium containing Pb(II), Cu(II) and Zn(II). The results revealed that the removal percent of Au(III) was much higher

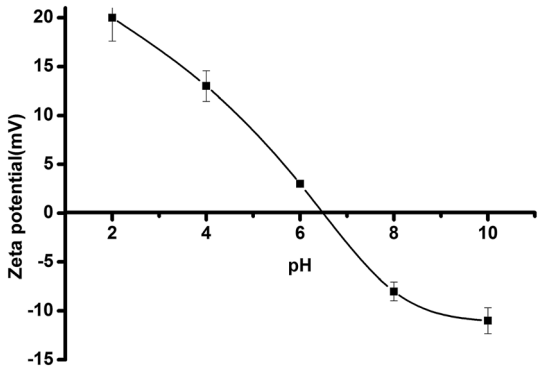

Fig. 6 Effect of pH on zeta potential values of TSC–SNC, TSC–SNC = 20 mg, $[Au^{3+}] = 100$ mg L^{-1}, adsorption time = 5 h.

than that of the other metal ions, indicating the TSC–SNC is a promising adsorbent for selective recovery of Au(III) from aqueous solutions (Fig. 7).

3.2.3 Adsorption isotherms. The experimental data of Au(III) on TSC–SNC was analyzed using Langmuir and Freundlich models. The Langmuir isotherm assumes a monolayer adsorption and all adsorption sites uniformly distributed on a homogeneous surface,[17] which can be expressed as:

$$C_e/q_e = 1/q_0K_L + C_e/q_0 \quad (3)$$

where C_e (mmol L^{-1}) is the equilibrium concentration of Au(III), q_e (mmol g^{-1}) is the adsorption capacity at equilibrium, K_L (L $mmol^{-1}$) and q_0 (mmol g^{-1}) are the Langmuir constants involved in adsorption rate and adsorption capacity. While the Freundlich isotherm presumes that the multilayer of the adsorption process occurs on a heterogeneous surface.[18] Freundlich isotherm can be expressed:

$$\ln q_e = \ln K_F + 1/n \ln C_e \quad (4)$$

where K_F and n are Freundlich constants.

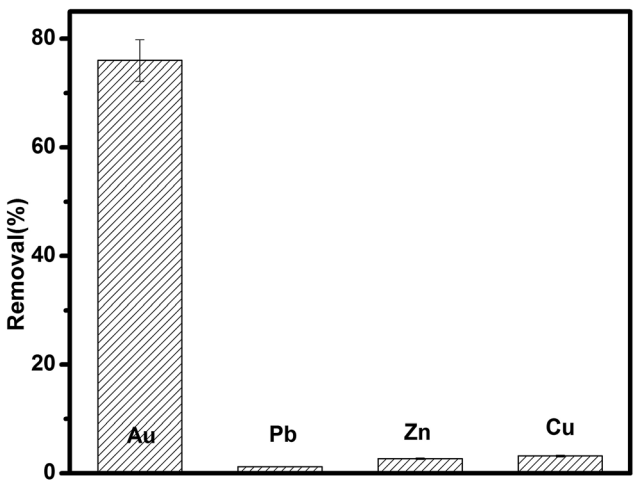

Fig. 7 Selective adsorption of TSC–SNC for Au(III). Ion concentration of Au(III), Cu(II), Zn(II) and Pb(II) is 100 mg L^{-1}, adsorption time = 5 h.

Table 1 Isotherm parameters for Au(III) adsorption on TSC–SNC

Isotherms	Parameters	R^2
Langmuir	$q_0 = 4.32$ mmol g^{-1} $K_L = 18.1$ L mmol^{-1}	0.991
Freundlich	$K_F = 4.4$ mmol g^{-1} $n = 5.7$	0.951

The adsorption data from Langmuir and Freundlich models were collected in Table 1. It can be seen that the Langmuir model (Fig. 8a) fits better than the Freundlich model (Fig. 8b). Therefore, the adsorption of Au(III) on TSC–SNC can be regarded as a monolayer adsorption, and the maximum adsorption capacity calculated from the Langmuir isotherm was 4.3 mmol g^{-1}. Table 2 reveals a comparison of adsorption capacity between the TSC–SNC adsorbent and other listed adsorbents reported in the literatures. As can be seen from Table 2, the as-prepared nanocomposite presents an excellent adsorption ability.

3.2.4 Adsorption kinetics. Adsorption kinetic can provide important information on the adsorption behaviors. The Lagergren pseudo-first-order and pseudo-second-order kinetic model were employed to study the adsorption kinetics of Au(III). These two kinetic models are given as:[23]

$$\ln(q_1 - q_t) = \ln(q_e) - k_1 t \quad (5)$$

$$t/q_t = 1/k_2 q_2^2 + t/q_2 \quad (6)$$

where q_1 represents the maximum adsorption capacity (mmol g^{-1}) for the pseudo first order adsorption, q_2 represents the maximum adsorption capacity (mmol g^{-1}) for the pseudo-second-order adsorption, q_t (mmol g^{-1}) represents the amounts of Au(III) adsorbed at any time (min). k_1 (min^{-1}) is the rate constant of the pseudo-first-order model and k_2 (g mmol^{-1} min^{-1}) is the pseudo-second-order rate constant.

The kinetic parameters and the correlation coefficients (R^2) were listed in Table 3. Pseudo-second-order model fitted better the adsorption kinetics due to the relative high R^2 (Fig. 9b). The value of q_2 calculated from the pseudo-second-order kinetic equation is more similar to the experimental value than that of q_1. It indicated that the kinetics of Au(III) adsorption onto TSC–SNC obeyed the pseudo-second-order model. The Lagergren pseudo-second-order kinetic model assumes that the rate-limiting step is the chemical adsorption.[24]

Table 2 Comparison of adsorption capacity of TSC–SNC with adsorbents reported in literature

Sorts of adsorbent	Adsorption capacity and corresponding references
Chelating resin	0.73 mmol g^{-1} (ref. 3) 2.23 mmol g^{-1} (ref. 19) 0.25 mmol g^{-1} (ref. 13) 53.6 mg mL^{-1} (ref. 32)
Chitosan	0.85 mmol g^{-1} (ref. 20) 0.35 mmol g^{-1} (ref. 21) 3.6 mmol g^{-1} (ref. 28) 30.95 mg g^{-1} (ref. 29) 198.5 mg g^{-1} (ref. 30)
Carbon	1.48 mmol g^{-1} (ref. 22) 1.15 mg g^{-1} (ref. 25) 108.34 mg g^{-1} (ref. 34) 1076.64 mg g^{-1} (ref. 37)
Polymer or gel	0.637 mmol g^{-1} (ref. 31) 2.8 mmol g^{-1} (ref. 33) 0.8 mmol g^{-1} (ref. 40)
Biosorbent	0.05 mol kg^{-1} (ref. 26) 0.45 mmol g^{-1} (ref. 35) 784 mg g^{-1} (ref. 36)
Nanoparticles	499.22 mg g^{-1} (ref. 27) 0.4 mmol g^{-1} (ref. 38) 208.3 mg g^{-1} (ref. 39)
TSC–SNC	4.3 mmol g^{-1} this study

Table 3 Kinetic models for Au(III) adsorption on TSC–SNC

Models	Model parameters	R^2
Pseudo-first-order	$q_1 = 1.6$ mmol g^{-1} $k_1 = 38.46$ min^{-1}	0.961
Pseudo-second-order	$q_2 = 2.3$ mmol g^{-1} $k_2 = 0.03$ g mmol^{-1} min^{-1}	0.991

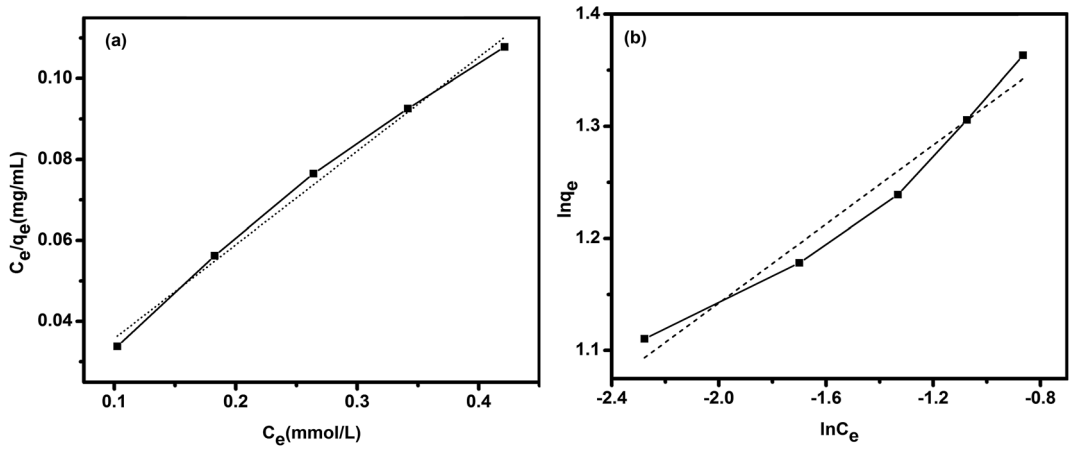

Fig. 8 Adsorption isotherms, (a) Langmuir model. (b) Freundlich model.

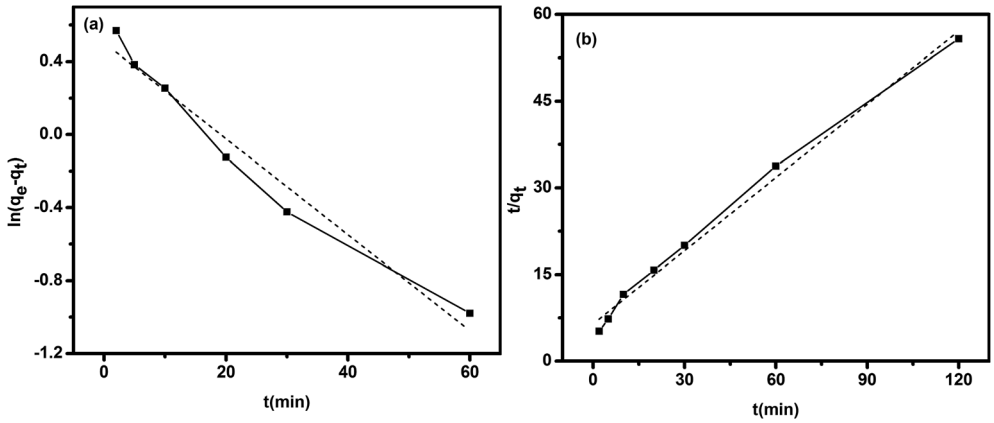

Fig. 9 Adsorption kinetic model (a) the pseudo-first-order adsorption kinetic model. (b) The pseudo-second-order adsorption kinetic model.

3.2.5 Adsorption mechanism of Au(III) onto TSC–SNC. To clarify the adsorption mechanism of Au(III) onto TSC–SNC, XPS studies of the adsorbent before and after the adsorption of Au(III) were carried out. In Fig. 2, the spectra of the Au(III) loaded TSC–SNC (defined as TSC–SNC–Au) appeared a new peak at about 88 eV corresponding to Au 4f, which indicated that Au(III) was adsorbed onto the surface of the adsorbent. And the peak at 202 eV corresponding to Cl 2p suggested that gold was adsorbed as chloride complex. The appearance of Au 4d peak at 353 eV indicated that a portion of Au(III) ions were adsorbed due to ionic interaction.[1]

The high resolution spectra of N 1s and S 2p of TSC–SNC and TSC–SNC–Au are shown in Fig. 10. The N 1s spectrum of TSC–SNC can be curve-fitted into peaks at 398.6, 399.4 and 400.1 eV, corresponding to C=N, –NH/–NH_2 and –NH_2^+ species, respectively. Fig. 10b shows that the binding energy of –NH/–NH_2 groups (400.2 eV) increased after Au(III) was adsorbed on the nanocomposite. This indicated that the amino groups were key factor for coordinating with Au(III). A broader peak of –NH_2^+ suggested that the most amino groups were protonated in acidic condition. The gold complex anions, therefore, can be adsorbed to the nanocomposite by ionic interaction.

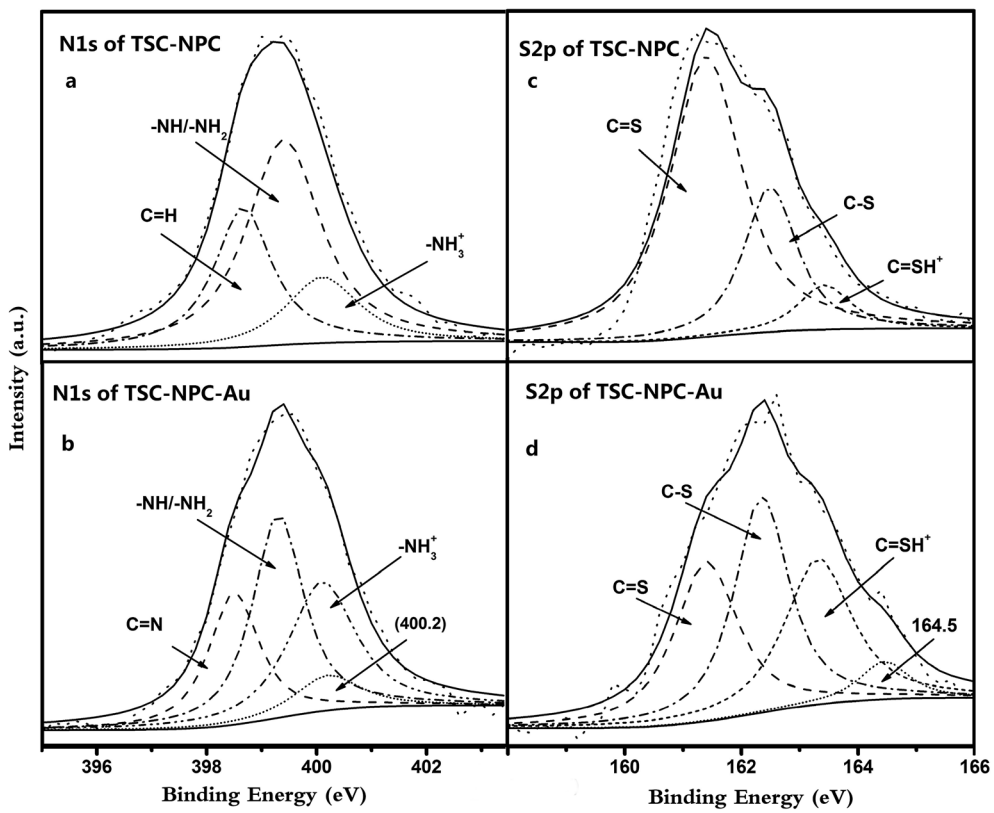

Fig. 10 The high-resolution core-level spectra of N 1s and S 2ps for TSC–SNC and TSC–SNC–Au.

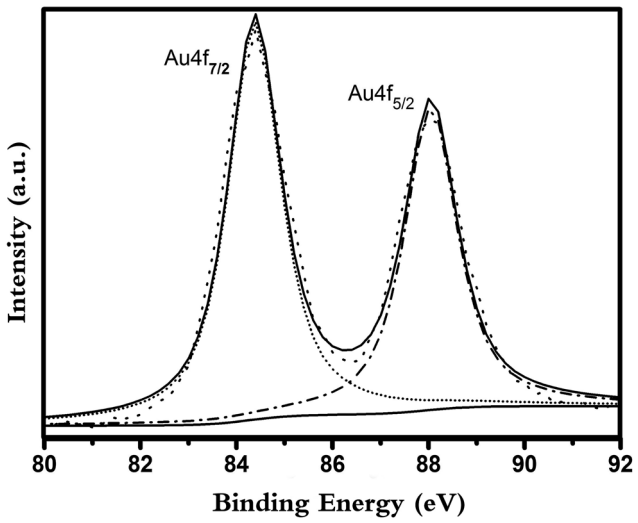

Fig. 11 The high-resolution core-level spectra of Au 4f in TSC–SNC–Au.

In Fig. 10c, the XPS spectra of S 2p were curve-fitted into three different component peaks at 161.4, 162.5 and 163.4 assigning to C═S, C–S and C═SH^+ species, respectively. After Au(III) adsorption, the C–S binding energy of a portion of C–S shifted from 162.5 to 164.5 eV, indicating that the thiol groups coordinated with Au(III). In addition, the protonation effect broadened the peak of C═SH^+, which indicated that the protonated thioamide groups were attracted gold complex anions.

The signal of Au 4f is presented in Fig. 11. The binding energy of Au 4f around 88.9 and 85.4 eV in TSC–SNC–Au were much lower than that in Au(III). This result indicated Au(III) accepted electrons in the chelating process. So we proposed two mechanisms of Au(III) ions adsorption, one is Au(III) complexing with the thiol and amino groups, the other is the ionic interaction between the protonated groups and the gold complex anions. The Au(III) adsorption is due to the synergistic effect of ionic interaction and chelation.

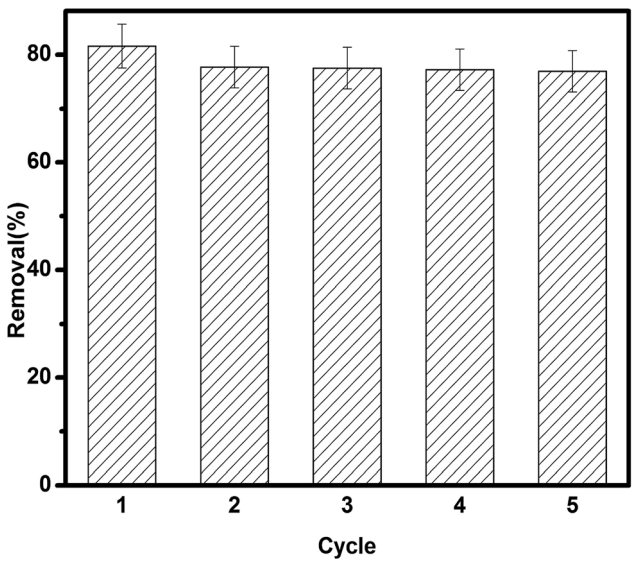

Fig. 12 Regeneration study of 5 cycles.

3.2.6 Desorption and recycling. The recycling of the adsorbent is very important to its practical application. Fig. 12 shows the Au(III) adsorption on the TSC–SNC in five successive cycles of desorption/adsorption process. It can be seen that there is slightly decrease of the removal percent of Au(III) after five cycles, indicating the TSC–SNC adsorbent have good recycling.

4. Conclusions

In conclusion, we have developed a procedure for selective removal of Au(III) from aqueous solution using thiosemicarbazide/nanosilica composite synthesized *via* cross-linking the thiosemicarbazide with glutaraldehyde onto the surface of the amino functionalized silica nanoparticles. The highest Au(III) uptake value was obtained for 4.3 mmol g^{-1} at pH 2. The TSC–SNC nanocomposite showed higher affinity toward Au(III) compared with other Pb(II), Cu(II) and Zn(II) ions. The Au(III) adsorption on TSC–SNC obeyed the pseudo-second-order kinetics model and the equilibrium data was well fitted by the Langmuir models. The high selective Au(III) adsorption indicates that a synergistic effect of ionic interaction and chelation exists between Au(III) and TSC–SNC nanocomposites. The adsorbent showed high durability and easy regeneration. Efforts in our group are being made to extend current work to applications in recovery of noble metal ions. We anticipate this TSC–SNC nanocomposites to find uses in the field of environmental protection and secondary resource recovery.

Conflicts of interest

There are no conflicts to declare.

Acknowledgements

The authors are grateful for the financial support from the National Natural Science Foundation (No. 51664037) and Research Fund for Advanced Talents (No. 163083).

References

1 L. J. Pang, R. Li, Q. H. Gao, J. T. Hu, Z. Xing, M. X. Zhang, M. H. Wang and G. Z. Wu, Functionalized and reusable polyethylene fibres for Au(III) extraction from aqueous solution with high adsorption capacity and selectivity, *RSC Adv.*, 2016, **6**, 87221–87229.

2 J. Jiang, Y. He, H. Gao and J. Wu, Solvent extraction of gold from alkaline cyanide solution with a tri-octylamine/tributyl phosphate/-heptane synergistic system, *Solvent Extr. Ion Exch.*, 2005, **23**, 113–129.

3 L. Guo, C. Liu, Z. Guo, L. Sun and J. Liu, Preparation of polyvinyl chloride-based thiosemicarbazide resin and its selective adsorption of Ag(I) and Au(III), *J. Dispersion Sci. Technol.*, 2012, **33**, 690–696.

4 K. Kashefi, J. M. Tor, K. P. Nevin and D. R. Lovley, Reductive precipitation of gold by dissimilatory Fe(III)-reducing bacteria and archaea, *Appl. Environ. Microbiol.*, 2001, **67**, 3275–3279.

5 A. Kargari, T. Kaghazchi, B. Mardangahi and M. Soleimani, Experimental and modeling of selective separation of gold(III) ions from aqueous solutions by emulsion liquid membrane system, *J. Membr. Sci.*, 2006, **279**, 389–393.

6 Q. Xu, P. Yin, G. Zhao, Y. Sun and R. Qu, Adsorption selectivity and dynamic adsorption behaviors of Cu(II), Ag(I), and Au(III) on silica gel encapsulated by amino functionalized polystyrene, *J. Appl. Polym. Sci.*, 2010, **117**, 3645–3650.

7 A. M. Donia, A. A. Atia and K. Z. Elwakeel, Gold(III) recovery using synthetic chelating resins with amine, thio and amine/mercaptan functionalities, *Sep. Purif. Technol.*, 2005, **42**, 111–116.

8 L. Zhang, Z. Li, X. Du and X. Chang, Activated carbon functionalized with 1-amino-2-naphthol-4-sulfonate as a selective solid-phase sorbent for the extraction of gold(III), *Microchim. Acta*, 2011, **174**, 391.

9 E. Ertan and M. Gülfen, Separation of gold(III) ions from copper(II) and zinc(II) ions using thiourea-formaldehyde or urea-formaldehyde chelating resins, *J. Appl. Polym. Sci.*, 2009, **111**, 2798–2805.

10 C. Mack, B. Wilhelmi, J. R. Duncan and J. E. Burgess, Biosorption of precious metals, *Biotechnol. Adv.*, 2007, **25**, 264–271.

11 P. K. Jal, S. Patel and B. K. Mishra, Chemical modification of silica surface by immobilization of functional groups for extractive concentration of metal ions, *Talanta*, 2004, **62**, 1005–1028.

12 P. A. Kumar, M. Ray and S. Chakraborty, Hexavalent chromium removal from wastewater using aniline formaldehyde condensate coated silica gel, *J. Hazard. Mater.*, 2007, **143**, 24–32.

13 L. S. Khabbaz, M. Hassanzadeh-Khayyat, P. Zaree, M. Ramezani, K. Abnous and S. M. Taghdisi, Detection of kanamycin by using an aptamer-based biosensor using silica nanoparticles, *Anal. Methods*, 2015, **7**, 8611–8616.

14 S. H. Araghi and M. H. Entezari, Amino-functionalized silica magnetite nanoparticles for the simultaneous removal of pollutants from aqueous solution, *Appl. Surf. Sci.*, 2015, **333**, 68–77.

15 T. A. Yousef, G. El-Reash, O. El-Gammal and R. A. Bedier, Synthesis, characterization, optical band gap, in vitro antimicrobial activity and DNA cleavage studies of some metal complexes of pyridyl thiosemicarbazone, *J. Mol. Struct.*, 2013, **1035**, 307–317.

16 A. Aydın, M. Imamoglu and M. Gulfen, Separation and recovery of gold(III) from base metal ions using melamine–formaldehyde–thiourea chelating resin, *J. Appl. Polym. Sci.*, 2008, **107**, 1201–1206.

17 L. Zhang, Y. Liu, S. Wang, B. Liu and J. Peng, Selective removal of cationic dyes from aqueous solutions by an activated carbon-based multicarboxyl adsorbent, *RSC Adv.*, 2015, **5**, 99618–99626.

18 R. Ii, S. C. Baxter, M. Bode, J. K. Berch, R. N. Shah and K. D. Shimizu, Application of the Freundlich adsorption isotherm in the characterization of molecularly imprinted polymers, *Anal. Chim. Acta*, 2001, **435**, 35–42.

19 A. M. Donia, A. A. Atia and K. Z. Elwakeel, Gold(III) recovery using synthetic chelating resins with amine, thio and amine/mercaptan functionalities, *Sep. Purif. Technol.*, 2005, **42**, 111–116.

20 A. Ramesh, H. Hasegawa, W. Sugimoto, T. Maki and K. Ueda, Adsorption of gold(III), platinum(IV) and palladium(II) onto glycine modified crosslinked chitosan resin, *Bioresour. Technol.*, 2008, **99**, 3801–3809.

21 K. Fujiwara, A. Ramesh, T. Maki, H. Hasegawa and K. Ueda, Adsorption of platinum(IV), palladium(II) and gold(III) from aqueous solutions onto L-lysine modified crosslinked chitosan resin, *J. Hazard. Mater.*, 2007, **146**, 39–50.

22 X. Chen, K. F. Lam, S. F. Mak and K. L. Yeung, Precious metal recovery by selective adsorption using biosorbents, *J. Hazard. Mater.*, 2011, **186**, 902–910.

23 J. Fu, Z. Chen, M. Wang, S. Liu, J. Zhang, J. Zhang, R. Han and Q. Xu, Adsorption of methylene blue by a high-efficiency adsorbent (polydopamine microspheres): kinetics, isotherm, thermodynamics and mechanism analysis, *Chem. Eng. J.*, 2015, **259**, 53–61.

24 L. Bai, H. Hu, W. Fu, J. Wan, X. Cheng, Z. Lei, L. Xiong and Q. Chen, Synthesis of a novel silica-supported dithiocarbamate adsorbent and its properties for the removal of heavy metal ions, *J. Hazard. Mater.*, 2011, **195**, 261–275.

25 M. R. Nabid, R. Sedghi, R. Hajimirza, H. A. Oskooie and M. M. Heravi, A nanocomposite made from conducting organic polymers and multi-walled carbon nanotubes for the adsorption and separation of gold(III) ions, *Microchim. Acta*, 2011, **175**, 315–322.

26 D. Parajuli, C. R. Adhikari, M. Kuriyama, H. Kawakita, K. Ohto, K. Inoue and M. Funaoka, Selective recovery of gold by novel lignin-based adsorption gels, *Ind. Eng. Chem. Res.*, 2006, **45**, 8–14.

27 P. Yin, C. Wang, Y. Yang, Y. Tian and Z. Yu, Thermodynamics and kinetics of Au(III) adsorption on silica gel chemically modified by diethylenetriamine bis(methylene phosphonic acid), *J. Chem. Eng. Data*, 2011, **56**, 450–457.

28 A. M. Donia, A. A. Atia and K. Z. Elwakeel, Recovery of gold(III) and silver(I) on a chemically modified chitosan with magnetic properties, *Hydrometallurgy*, 2007, **87**, 197–206.

29 W. S. Wan Ngah and K. H. Liang, Adsorption of gold(III) ions onto chitosan and N-carboxymethyl chitosan: equilibrium studies, *Ind. Eng. Chem. Res.*, 1999, **38**, 1411–1414.

30 F. Li, C. Bao, J. Zhang, Q. Sun, W. Kong, X. Han and Y. Wang, Synthesis of chemically modified chitosan with 2,5-dimercapto-1,3,4-thiodiazole and its adsorption abilities for Au(III), Pd(II), and Pt(IV), synthesis of chemically modified chitosan with 2,5-dimercapto-1,3,4-thiodiazole and its adsorption abilities for Au(III), Pd(II), and Pt(IV), *J. Appl. Polym. Sci.*, 2009, **113**, 1604–1610.

31 H. Tokuyama and A. Kanehara, Temperature swing adsorption of gold(III) ions on poly(N-isopropylacrylamide) gel, *React. Funct. Polym.*, 2007, **67**, 136–143.
32 N. V. Nguyen, J. Jeong, M. K. Jha, J. Lee and K. Osseo-Asare, Comparative studies on the adsorption of Au(III) from waste rinse water of semiconductor industry using various resins, *Hydrometallurgy*, 2010, **105**, 161–167.
33 J. Sanchez, M. Hidalgo and V. Salvado, The selective adsorption of gold(III) and palladium(II) on new phosphine sulphide-type chelating polymers bearing different spacer arms: equilibrium and kinetic characterization, *React. Funct. Polym.*, 2001, **46**, 283–291.
34 L. Liu, S. Liu, Q. Zhang, C. Li, C. Bao, X. Liu and P. Xiao, Adsorption of Au(III), Pd(II), and Pt(IV) from aqueous solution onto graphene oxide, *J. Chem. Eng. Data*, 2013, **58**, 209–216.
35 R. Qu, C. Sun, M. Wang, C. Ji, Q. Xu, Y. Zhang, C. Wang, H. Chen and P. Yin, Adsorption of Au(III) from aqueous solution using cotton fiber/chitosan composite adsorbents, *Hydrometallurgy*, 2009, **100**, 65–71.
36 X. Liao, M. Zhang and B. Shi, Collagen-fiber-immobilized tannins and their adsorption of Au(III), *Ind. Eng. Chem. Res.*, 2004, **43**, 2222–2227.
37 L. Liu, C. Bao, Q. Jia, P. Xiao, X. Liu and Q. Zhang, Preparation and characterization of chitosan/graphene oxide composites for the adsorption of Au(III) and Pd(II), *Talanta*, 2012, **93**, 350–357.
38 K. F. Lam, C. M. Fong, K. L. Yeung and G. Mckay, Selective adsorption of gold from complex mixtures using mesoporous adsorbents, *Chem.–Eng. J.*, 2008, **145**, 185–195.
39 Y. Yu, J. Addai-Mensah and D. Losic, Chemical functionalization of diatom silica microparticles for adsorption of gold(III) ions, *J. Nanosci. Nanotechnol.*, 2011, **11**, 10349–10356.
40 P. Yin, Q. Xu, R. Qu and G. Zhao, Removal of transition metal ions from aqueous solutions by adsorption onto a novel silica gel matrix composite adsorbent, *J. Hazard. Mater.*, 2009, **169**, 228–232.